



Cite this: DOI: 10.1039/d6sc01992g

All publication charges for this article have been paid for by the Royal Society of Chemistry

# Magnesium(0) complexes and their reduction reactions with binary transition metal carbonyls

Yixiao Jiang,<sup>a</sup> Maryam Niksefat,<sup>a</sup> Sophie G. Unsworth,<sup>a</sup> Joseph M. Parr,<sup>a</sup> Matthew J. Evans<sup>ab</sup> and Cameron Jones<sup>ib</sup>\*<sup>a</sup>

Three very bulky  $\beta$ -diketimine protio-ligands ( $^{\text{Ar}}\text{NacnacH}$ ,  $\{(\text{Ar})\text{N}=\text{C}(\text{Bu})_2\text{CH}_2$ , Ar = 2,4,6-tricyclohexylphenyl TCHP; 2,6-dicyclohexylphenyl DCHP; TCHP/Dip, Dip = 2,6-diisopropylphenyl) have been synthesised. These have been used to prepare monomeric, three-coordinate  $\beta$ -diketiminato magnesium iodide complexes,  $[(^{\text{Ar}}\text{Nacnac})\text{MgI}]$  (Ar = TCHP **1**, DCHP **3**, or TCHP/Dip **5**). Sodium metal reduction of **1** afforded the thermally robust anionic magnesium(0) complex  $[(^{\text{TCHP}}\text{Nacnac})\text{Mg}]\text{Na}_2$  **6** in good yield. In contrast, reduction of less bulky  $[(^{\text{DCHP}}\text{Nacnac})\text{MgI}]$  **3** gave a mixture of unknown products, whilst reduction of  $[(^{\text{TCHP/Dip}}\text{Nacnac})\text{MgI}]$  **5** yielded the mixed oxidation state magnesium compound,  $[(^{\text{TCHP/Dip}}\text{Nacnac})\text{Mg}]_2\text{Mg}$  **7**. The related compound  $[(^{\text{TCHP}}\text{Nacnac})\text{Mg}]_2\text{Mg}$  **8**, was prepared by reduction of a 2 : 1 mixture of  $[(^{\text{TCHP}}\text{Nacnac})\text{MgI}]$  **1** and  $\text{MgI}_2$ . Computational analyses of **6** and **8** reveal their electronic structures to be comparable to those of previously reported analogues of these compounds. Reduction reactions between magnesium(0) compound **6** and the neutral groups **6** and **7** transition metal carbonyls,  $\text{Cr}(\text{CO})_6$ ,  $\text{Mo}(\text{CO})_6$  and  $\text{Mn}_2(\text{CO})_{10}$ , gave a series of complexes  $[(^{\text{TCHP}}\text{Nacnac})\text{Mg}]_2\{\mu\text{-M}_2(\text{CO})_n\}$  ( $n = 10$ , M = Cr **9** or Mo **10**;  $n = 8$ , M = Mn **11**) which incorporate metal–metal single (**9** and **10**) or double (**11**) bonded metal carbonyl fragments. In contrast, reduction of  $\text{Fe}(\text{CO})_5$  with **6** yielded  $[(^{\text{TCHP}}\text{Nacnac})\text{Mg}]\text{Na}\{\text{Fe}(\text{CO})_4\}_2$  **12** which does not possess an Fe–Fe bond, and can be viewed as an analogue of Collman's reagent,  $\text{Na}_2[\text{Fe}(\text{CO})_4]$ , in which one  $\text{Na}^+$  cation has been replaced by a  $[(^{\text{TCHP}}\text{Nacnac})\text{Mg}]^+$  unit.

Received 10th March 2026  
Accepted 17th April 2026

DOI: 10.1039/d6sc01992g

rsc.li/chemical-science

## Introduction

In contrast to the chemistry of low oxidation state p-block metal compounds, which has developed since the 1970s,<sup>1</sup> it was not until 2007 that the first examples of well-defined, room temperature stable, low oxidation state s-block complexes, *e.g.* **I** (Fig. 1), were reported.<sup>2</sup> These dimagnesium(i) systems were kinetically stabilised by bulky *N,N*-chelating  $\beta$ -diketiminate or guanidinate ligands, and were shown to possess unsupported Mg–Mg covalent bonds. Since this report, nearly 50 other compounds bearing Mg–Mg covalent bonds have come forward,<sup>3</sup> including systems that are neutral or dianionic, *e.g.* **II**,<sup>4</sup> and in which the magnesium centres exhibit coordination numbers ranging from two to four. The high reactivity and solubility of dimagnesium(i) compounds have lent them to wide use as specialist reducing reagents in many areas of inorganic and organic synthesis, which has allowed entry to numerous compound types that are not accessible using more traditional reducing agents, such as alkali metals or  $\text{KC}_8$ .<sup>3</sup>

The realisation that low oxidation state magnesium compounds can be tamed has inspired chemists to pursue other challenging targets in this realm.<sup>5</sup> Arguably, of most importance here is the first magnesium(0) complex, **III**, reported by Harder and co-workers in 2021.<sup>6</sup> Like **I**, this was prepared by alkali metal reduction of a  $\beta$ -diketiminato magnesium(i) iodide precursor complex,  $[(^{\text{Dipep}}\text{Nacnac})\text{MgI}]$  ( $^{\text{Dipep}}\text{Nacnac} = \{[(\text{Dipep})\text{NC}(\text{Bu})_2\text{CH}]^-\}$  Dipep = 2,6-di(3-pentyl)phenyl). However, in the case of the formation of **III**, the considerably bulkier Dipep *N*-substituents, and *tert*-butyl backbone groups, presumably prevented homocoupling of magnesium(i) radical intermediates to give an Mg–Mg bond, and instead allowed a further reduction of those intermediates to give the magnesium(0) complex. It is noteworthy that solutions of **III** slowly decompose at room temperature, *via* partial disproportionation, to give the unusual mixed-valence species, **IV**. Since the initial report on **III**, this compound has begun to prove its worth as a reagent for the preparation of Mg–E (E = group 2 metal, group 14 element, Yb) bonded species, synthetically useful redox active heterobimetallic inverse crown compounds, and for the reduction of organic substrates.<sup>7–9</sup>

In recent years, we have developed a range of anionic and dianionic *N,N*-chelating ligands that incorporate the very bulky 2,4,6-tricyclohexylphenyl (TCHP) group at their *N*-centres. Like the Dipep substituted  $\beta$ -diketiminate units in **III**, these sterically imposing ligands can provide considerably greater kinetic

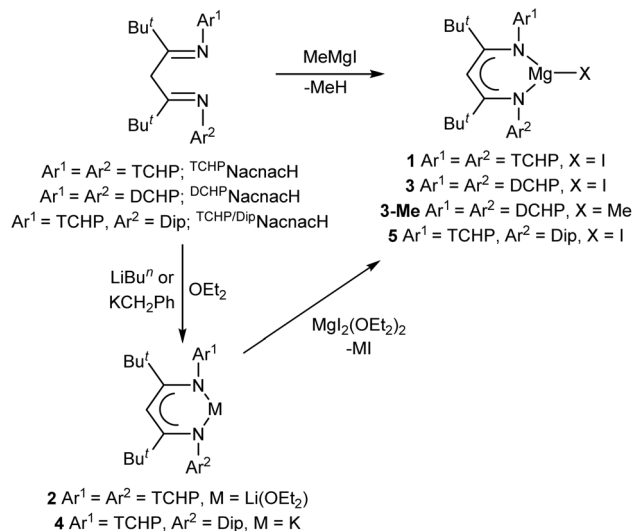
<sup>a</sup>School of Chemistry, Monash University, PO Box 23, VIC, 3800, Australia; Web: <http://www.monash.edu/science/research-groups/chemistry/jonesgroup>

<sup>b</sup>College of Science and Engineering, Flinders University, Bedford Park, SA, 5042, Australia. E-mail: cameron.jones@monash.edu





Fig. 1 Previously reported examples of magnesium(i) and magnesium(0) compounds (Mg–Mg bond lengths in parentheses). Dip = 2,6-diisopropylphenyl, TCHP = 2,4,6-tricyclohexylphenyl, Di pep = 2,6-di(3-pentyl)phenyl.



Scheme 1 Synthesis of compounds 1–5; DCHP = 2,6-dicyclohexylphenyl.

stabilisation to formed complexes than do their 2,6-diisopropylphenyl (Dip) substituted counterparts (e.g. as in I). This has allowed us access to a raft of new compound types, including the first examples of anionic calcium<sup>10</sup> and magnesium–dinitrogen complexes,<sup>11</sup> stabilised by bulky TCHP adorned xanthene-bridged diamide ligands (cf. II). With respect to low oxidation state  $\beta$ -diketiminate-magnesium compounds,

we have also prepared, and examined the chemistry of, the neutral dimagnesium(i) compound V.<sup>12</sup> Although this is structurally analogous to I, its Mg–Mg bond length (3.021(1) Å) is considerably greater than that of its Dip substituted counterpart (2.846(1) Å), due to the bulk of the ligand in V. In fact, the Mg–Mg bond length in V is close to that in the Di pep substituted species VI (3.051(1) Å),<sup>13</sup> which implies similar steric profiles for the  $\beta$ -diketiminate ligands in V and VI. In consideration of this, and the emerging synthetic utility of III, we were keen to develop the TCHP substituted analogue of the bulky  $\beta$ -diketiminate ligand in III (and related  $\beta$ -diketimines), in order to assess whether this could kinetically stabilise new magnesium(0) complexes (cf. III and IV). Herein, we report the positive results of our efforts in this direction, and additionally describe reductions of a series of binary transition metal carbonyl compounds with an anionic magnesium(0) complex.

## Results and discussion

### Magnesium(0) and mixed oxidation state magnesium (Mg<sup>0</sup>/Mg<sup>I</sup>) compounds

At the outset, three new bulky  $\beta$ -diketimine pro-ligands, all bearing *tert*-butyl backbone substituents, were synthesised in good yield *via* a protocol established by Budzelaar and co-workers (see SI for full details).<sup>14</sup> Two of these were symmetrically *N*-substituted with either TCHP or related DCHP (2,6-dicyclohexylphenyl) groups, *viz.* TCHP/NacnacH and DCHP/NacnacH, respectively (Scheme 1). A third unsymmetrical  $\beta$ -diketimine, TCHP/Dip/NacnacH, incorporates both TCHP and Dip *N*-



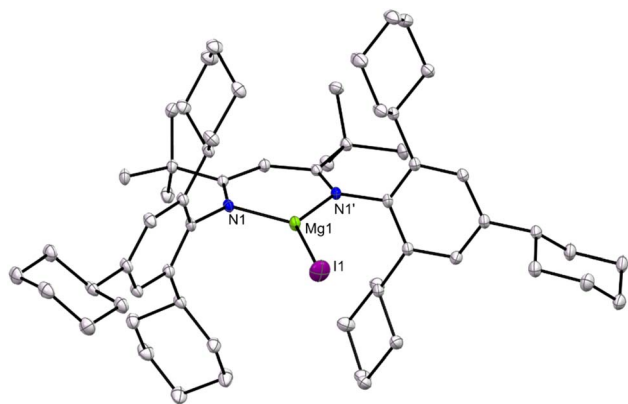
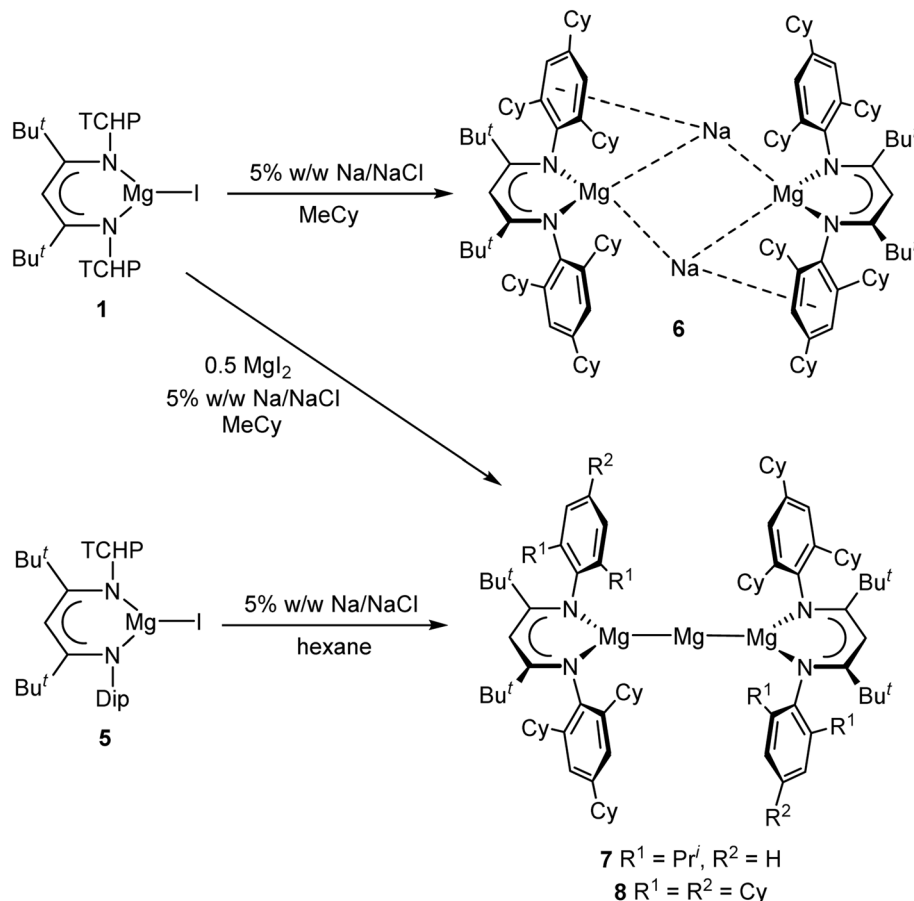


Fig. 2 Molecular structure of **1** (25% thermal ellipsoids; hydrogen atoms omitted). Selected bond lengths (Å) and angles (°): I(1)–Mg(1) 2.5927(11), Mg(1)–N(1) 1.9984(18), N(1)–Mg(1)–N(1) 97.40(10), N(1)–Mg(1)–I(1) 131.30(5).

substituents. NMR spectroscopic studies on the three  $\beta$ -diketimines indicated that they exist solely as their diimine tautomers in solution (as depicted in Scheme 1), in that there is no evidence for them being in equilibrium with measurable amounts of their ene-amine tautomers,  $\text{ArN}=\text{C}(\text{Bu}^t)\text{C}(\text{H})\text{C}(\text{Bu}^t)\text{N}(\text{H})\text{Ar}$ . Furthermore, heating solutions of the  $\beta$ -diketimines did not lead to tautomerisations. This is also the case for the

bulky  $\beta$ -diketimine used to prepare **III**, *viz.*  $\text{Dipe}^{\text{P}}\text{NacnacH}$ ,<sup>15</sup> whereas less bulky  $\beta$ -diketimines, such as that used in the synthesis of **I** (*viz.*  $\text{Dip}^{\text{P}}\text{NacnacH}$ ), are usually obtained in their ene-amine form. The solid-state structures of  $\text{D}^{\text{CHP}}\text{NacnacH}$  and  $\text{T}^{\text{CHP}}\text{Dip}^{\text{P}}\text{NacnacH}$  were confirmed by X-ray crystallographic studies, full details of which can be found in the SI.

With the three new  $\beta$ -diketimines in hand, synthetic routes to  $\beta$ -diketiminato magnesium(II) iodide compounds, as potential precursors to magnesium(0) complexes, were developed. In the case of  $\text{T}^{\text{CHP}}\text{NacnacH}$ , its deprotonation with the Grignard reagent  $\text{MeMgI}$  afforded a high isolated yield (80%) of colorless crystalline **1** (Scheme 1). The compound can alternatively be prepared in moderate yield (50%) by reaction of the lithium salt **2** (see SI for synthesis and full characterisation) with  $\text{MgI}_2(\text{-OEt}_2)_2$ . As an aside, it is noteworthy that aqueous quenching of **2** gave  $\text{T}^{\text{CHP}}\text{NacnacH}$ , but in this case as its ene-amine tautomer, rather than in its diimine form. This was spectroscopically and crystallographically characterised (see SI for full details), and shown not to tautomerise to its diimine form in solution, even at 60 °C. Similar to the formation of **1**, treating  $\text{D}^{\text{CHP}}\text{NacnacH}$  with  $\text{MeMgI}$  gave the corresponding magnesium iodide complex **3**, but this consistently co-crystallised with *ca.* 50% of the methyl magnesium complex **3-Me**, and the two products could not be separated. In this regard, analogous magnesium methyl/halide co-crystallised product mixtures have been



Scheme 2 Synthesis of compounds **6–8**.



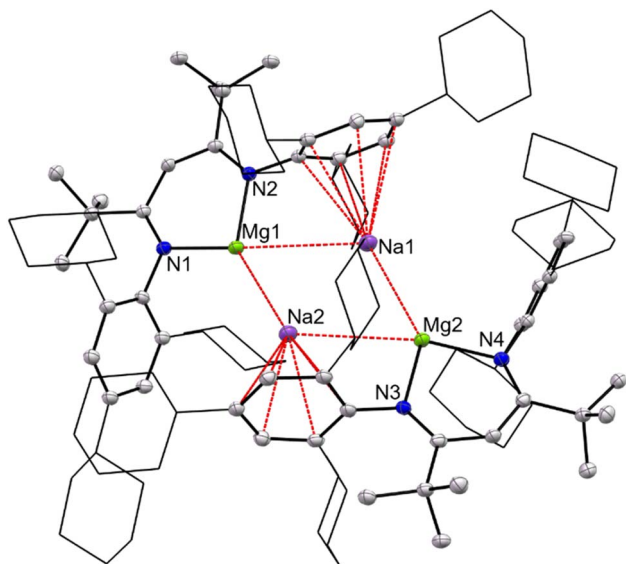


Fig. 3 Molecular structure of **6** (25% thermal ellipsoids; hydrogen atoms omitted; cyclohexyl groups shown as wireframe for clarity). See text for relevant bond lengths.

previously reported for reactions between very bulky  $\beta$ -diketiminates and methyl Grignard reagents.<sup>16</sup> In attempts to counter this problem, reactions of lithium or potassium salts of  $\text{D}^{\text{CHP}}\text{Nacnac}$  with  $\text{MgI}_2(\text{OEt}_2)_2$  were carried out, but these did not lead to tractable products. In contrast, deprotonation of the unsymmetrical  $\beta$ -diketimine,  $\text{T}^{\text{CHP/Dip}}\text{NacnacH}$ , with benzyl potassium gave the potassium salt **4**, which was subsequently reacted with  $\text{MgI}_2(\text{OEt}_2)_2$  to give a good isolated yield (66%) of the magnesium iodide complex **5**.

Compounds **1**, **3** and **5** are thermally stable solids. Their NMR spectra are consistent with their proposed formulations, which were confirmed by X-ray crystallographic structure determinations. The three compounds are structurally analogous, so only the molecular structure of **1** is depicted in Fig. 2, while those for **3** and **5** can be found in the SI. Compound **1** is monomeric in the solid-state, with its Mg centre exhibiting a trigonal planar coordination environment and a terminal iodide ligand. The facts that it does not dimerise through bridging iodides, and does not form an adduct with diethyl ether, despite being prepared in the presence of that solvent, are testament to the steric bulk of the  $\text{T}^{\text{CHP}}\text{Nacnac}$  ligand. Only a handful of monomeric, three-coordinate  $\beta$ -diketiminato magnesium iodide complexes are known, which include  $[(\text{Dip}^{\text{EP}}\text{Nacnac})\text{MgI}]$ .<sup>15,17</sup> The metrical parameters associated with the magnesium centre in that compound are almost identical to those for **1**.

In the next phase of this study, reductions of the magnesium(II) iodide precursor complexes **1**, **3** and **5** were investigated. Given that the reducing agent 5% w/w Na/NaCl, originally developed by our group,<sup>18</sup> was successfully used in the preparation of magnesium(0) complex **III**, it was also chosen for this study. Reduction of **1** with an excess of 5% w/w Na/NaCl in either aromatic or aliphatic solvents led to magnesium(0) complex **6** as deep red crystals in isolated yields of up to 85% (*cf.* isolated yield of **III** = 48%), after work-up

(Scheme 2). The compound is thermally stable at room temperature, and does not decompose in the solid-state below 170 °C. It is stable in benzene and methylcyclohexane solutions for days at room temperature, but when these solutions are heated to >70 °C the compound slowly decomposes to the protonated ligand  $\text{T}^{\text{CHP}}\text{NacnacH}$ , and other unidentified products. This is in contrast to **III**, benzene solutions of which slowly decompose at room temperature, and more rapidly at 56 °C, to give the mixed oxidation state compound **IV** in low yield.<sup>6</sup> Accordingly, the higher yield and greater thermal stability of **6** vs. **III**, should make it a suitable alternative to **III** in further reactivity studies that require magnesium(0) reagents. Although it cannot be sure what the mechanism of formation of **6** is, it seems likely that reduction of **1** initially gives the magnesium(I) radical,  $[(\text{T}^{\text{CHP}}\text{Nacnac})\text{Mg}^\cdot]$ , which is sterically prevented from undergoing a homo-coupling reaction to yield an *N,N*-chelated dimagnesium(I) compound. Instead, the radical is further reduced with sodium to give **6**.

Attention then turned to the reduction of **3** and **5** with excess 5% w/w Na/NaCl. In the case of **3** only complex mixtures of products were returned, which likely results from the unavoidable contamination of **3** with **3-Me**. In contrast, reduction of hexane solutions of the unsymmetrical precursor **5**, afforded a good yield (60%) of the dark red compound **7**, in which the central Mg centre has a formal oxidation state of zero, whilst the terminal Mg atoms are in the +1 oxidation state (Scheme 2). While there was no evidence for the presence of a magnesium(0) complex analogous to **6** in the reaction mixture, it possibly exists as a transient intermediate, which rapidly decomposes *via* partial disproportionation to **7**. This is similar to the proposed formation of **IV**. It also seems likely that the decomposition to **7** occurs much more rapidly, due to the lesser steric protection provided by the unsymmetrical  $\beta$ -diketiminato ligand in this case. In light of the formation of **7**, we wondered if we could devise a rational route to its  $\text{T}^{\text{CHP}}\text{Nacnac}$  coordinated analogue. To this end, we reduced a 2 : 1 mixture of **1** and  $\text{MgI}_2$  in methylcyclohexane, with 5% w/w Na/NaCl, which gave a good isolated yield (76%) of deep-red **8** after recrystallisation of the crude product mixture from hexane.

As is the case for **6**, compounds **7** and **8** show no signs of decomposition in the solid-state or in solution at room temperature over several days. The NMR spectra of **6** imply a symmetrical structure in solution, which contrasts with the lower symmetry aryl coordinated, sodium bridged structure found in the solid-state (see below). It is likely that this is due to fast exchange between Na-coordinated and uncoordinated arene rings in solution, as was suggested for analogous compound **III**.<sup>6</sup> The NMR spectra of the mixed oxidation state compounds **7** and **8** are consistent with their solid-state structures, though those for **7** are more complex, as would be expected given the unsymmetrical nature of the  $\beta$ -diketiminato ligands in that compound.

The X-ray crystal structure of **6** was determined, and its molecular structure is depicted in Fig. 3. This shows it to be structurally analogous to **III** in the solid-state. That is, it involves two formally anionic  $[(\text{T}^{\text{CHP}}\text{Nacnac})\text{Mg}^{0-}]$  fragments bridged by two sodium cations that are each  $\eta^6$ -coordinated by the central





Fig. 4 Molecular structures of **7** (top) and **8** (bottom) (25% thermal ellipsoids; hydrogen atoms omitted; cyclohexyl and isopropyl groups shown as wireframe for clarity). See text for relevant bond lengths and angles.

arene ring of a TCHP *N*-substituent. The Mg $\cdots$ Mg separation in **6**, 5.812(3) Å, is comparable to that in **III** (5.7792(5) Å), and is well outside what would be expected for the presence of any bonding interaction between the two magnesium centres. In contrast, the Na $\cdots$ Na separation in **6** (3.303(2) Å) is significantly longer than that in **III** (3.1521(8) Å), and as has been determined for that compound, there is likely no significant bonding interaction between the two alkali metals, as confirmed by DFT calculations (see below). An inspection of the Mg $\cdots$ Na distances in **6** reveal that the two shorter distances (Mg(1)–Na(2) 3.154(2) Å, Mg(2)–Na(1) 3.217(2) Å) are close to the equivalent distances in centrosymmetric **III**, 3.1216(7) Å, and are suggestive of bonding interactions between the metal pairs.

The molecular structures of the mixed oxidation state magnesium compounds **7** and **8** are shown in Fig. 4. They are both essentially isostructural with **IV**, and exhibit Mg–Mg bond lengths (**7** 2.828(2) Å, **8** 2.840(1) Å) that are close to those in **IV**

(2.8876(5) Å), and are very similar to those reported for unsupported Mg–Mg bonds in the majority of neutral dimagnesium(i) compounds, e.g. 2.8457(8) Å in **I**.<sup>2</sup> One notable difference between **7** and **8** is that in **8** the <sup>TCHP</sup>Nacnac ligands chelate the Mg(i) centres in a near symmetrical fashion, leading to the  $\beta$ -diketiminato backbone HC-carbon centre being close to linear with the Mg–Mg bond, i.e. C–Mg(1)–Mg(2) = 174.93(2)°. In contrast, the equivalent angle in **7**, (C–Mg(1)–Mg(2) 153.79(2)°), is considerably narrower. This arises from the unsymmetrical nature of the <sup>TCHP/Dip</sup>Nacnac ligand in the latter, which leads to the two smaller Dip groups “sandwiching” the central Mg(2) centre, but with an average Mg $\cdots$ C<sub>Ar</sub> distance (3.73 Å) that is not suggestive of any meaningful bonding interactions. A similar arrangement is not possible in **8** due to the considerable steric bulk of its <sup>TCHP</sup>Nacnac ligands. It is noteworthy that the equivalent C–Mg–Mg angle in **IV**, 164.77°, is nearly mid-way between those in **7** and **8**, which may give an indication of the magnitude of steric interactions between the two Nacnac ligands in each compound.

DFT calculations (B3PW91) were employed to probe the electronic structure and bonding of **6–8** in the gas phase. The geometries of the compounds optimised to be close to those of their solid-state structures. Natural Bond Orbital (NBO) and Atoms in Molecules (AIM) analyses of the geometry optimised compounds were carried out, and key data are summarised for **6** and **8** in Fig. 5 (see SI for data on **7**). The computed data for the two compounds closely match those obtained for **III** and **IV**,<sup>6</sup> so will not be discussed in detail here. However, it is worth noting that in the case of **6**, the HOMO and HOMO–1 are largely associated with the Mg centres and the Mg<sub>2</sub>Na<sub>2</sub> core of the molecule, respectively; while the LUMO is ligand based (Fig. S108). Like **III**, the data imply electron rich Mg<sup>0</sup> centres in **6**, which have essentially ionic interactions with the <sup>TCHP</sup>Nacnac ligands. The Natural Population Analysis (NPA) charges on the Mg and Na centres are higher and lower than would be expected for those metals in their 0 and +1 oxidation states, respectively (*viz.* Mg: +0.59 mean and Na: +0.43 mean; *cf.* +0.57 and +0.50 for **III**; *cf.* Bader charges for **6**: +0.45 mean and +0.71 mean), and point towards charge transfer from the Mg atoms to the Na cations. This is borne out by significant Wiberg Bond Index (WBI) values for the short, and to a lesser extent the long, Mg $\cdots$ Na interactions in the compound (*viz.* 0.424 mean and 0.088 mean respectively; *cf.* 0.354 and 0.105 for **III**). Consistent with this observation is the presence of bond critical points lying on all four Mg $\cdots$ Na bond paths in the Laplacian distribution plot of **6** (see Fig. S112).

For compound **8**, the HOMO and HOMO–1 are associated with bonding interactions over the linear Mg<sub>3</sub> fragment, while the LUMO is delocalised over the <sup>TCHP</sup>Nacnac ligands (see Fig. S110). Within that fragment, the two formally Mg<sup>I</sup> centres possess higher NPA charges (+0.774 and +0.801) than does the central Mg<sup>0</sup> atom (+0.408). The WBI values for the two Mg–Mg pairs (0.497 mean) are consistent with single covalent bonds. One difference between **8** and **IV** is the fact that Non-Nuclear Attractors (NNAs) were not found on the Mg–Mg vectors in the former, whereas they were in the latter,<sup>6</sup> and in the related dimagnesium(i) compound **I**.<sup>19</sup> In this respect, it should be noted



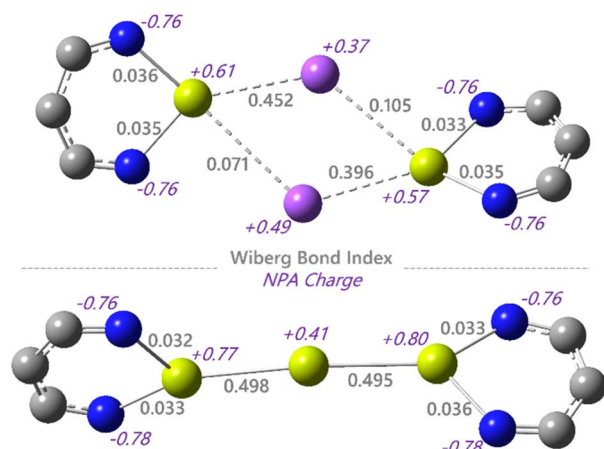


Fig. 5 Select NBO data for **6** (top) and **8** (bottom). Wiberg Bond Indices (WBIs) are listed in bold, with natural population analysis (NPA) charge data in purple text. Colour code: carbon = grey; nitrogen = blue; magnesium = yellow; and sodium = purple. Tricyclohexylphenyl and *tert*-butyl groups omitted for clarity.

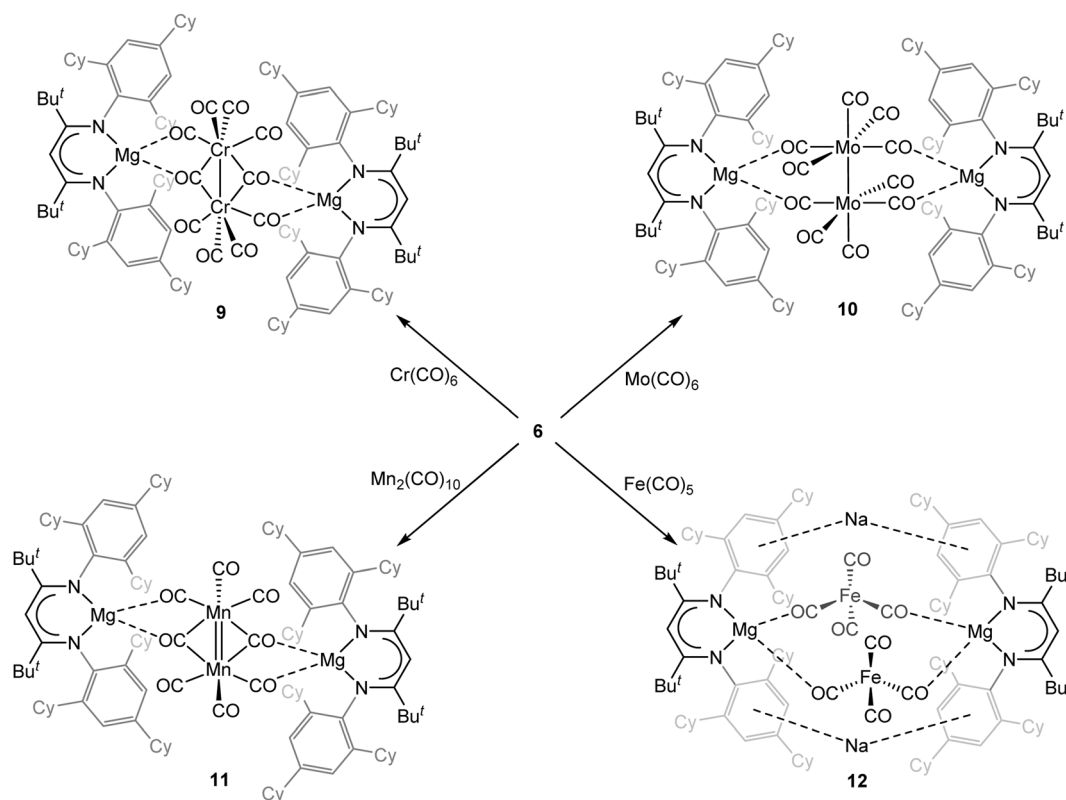
that the AIM calculations on **8** were performed at the same level of theory as those that located NNAs in **IV**.

### Reactions of a magnesium(0) compound with binary transition metal carbonyls

In recent years, we have explored the reductive homologation of carbon monoxide using either dimagnesium(i) compounds or masked magnesium(i) complexes as the reducing agent. These

studies have led to a series of magnesium coordinated oxocarbon anions, *e.g.*  $[C_nO_n]^{2-}$  ( $n = 2, 3$  or  $4$ )<sup>12,20</sup> and  $[C_6O_6]^{6-}$ ,<sup>21</sup> which have highlighted the possibility of using magnesium(i) compounds for the Fischer–Tropsch like formation of value-added organic products from the  $C_1$  feedstock gas, CO. In some cases, these reactions have required the presence of binary transition metal carbonyls as catalysts,<sup>21</sup> in order to increase product yield and selectivity. Accordingly, it seemed worthwhile to explore the reactivity of magnesium(0) compound **6** towards CO and/or transition metal carbonyls for sake of comparison with similar reactions involving dimagnesium(i) compounds. Another motivation for this investigation was the fact that, to the best of our knowledge, similar reactions with the only other magnesium(0) compound **III** have not been reported.

In the first instance, solutions of compound **6** in cyclohexane or benzene were stirred under an atmosphere of CO at room temperature. This led to rapid reactions which generated complex product mixtures, the components of which could not be identified. As a result, attention turned to reactions of **6** with the neutral groups 6–8 transition metal carbonyls,  $Cr(CO)_6$ ,  $Mo(CO)_6$ ,  $Mn_2(CO)_{10}$  or  $Fe(CO)_5$ , as potential sources of CO, under atmospheres of  $N_2$ . In all cases, no CO homologation reactions were observed. Instead, reduction of the metal carbonyl occurred, leading to products **9–12**, incorporating anionic metal carbonyl fragments (Scheme 3). The nature of the by-products from the reactions that gave sodium free **9–11** is not known, but it is possible that sodium salts of oxocarbon dianions, *i.e.*  $Na_2[C_nO_n]$ , are generated. Furthermore, it is



Scheme 3 Synthesis of compounds **9–12**.



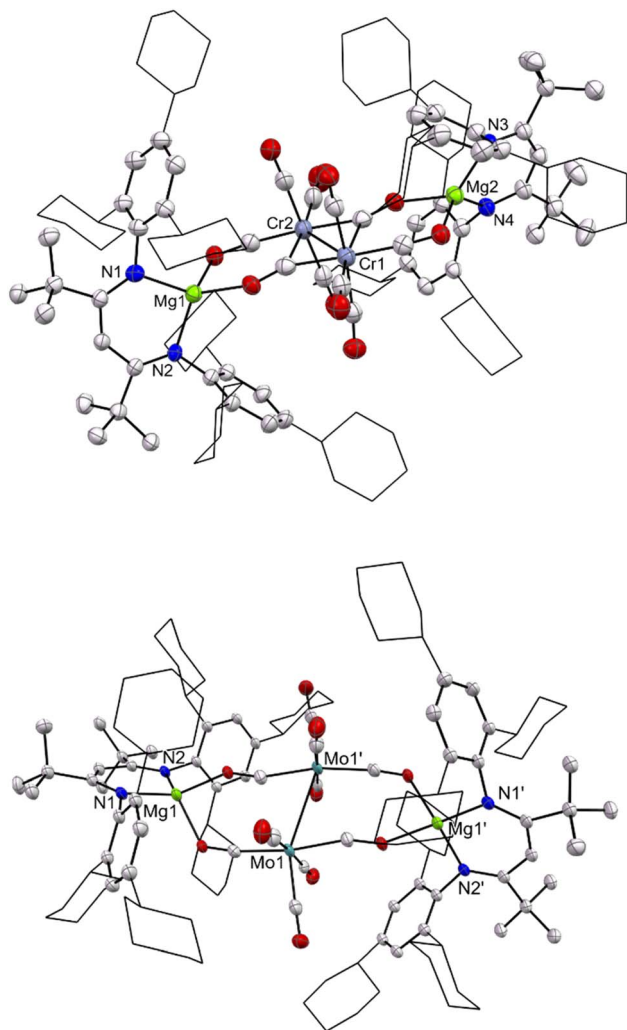


Fig. 6 Molecular structures of **9** (top) and **10** (bottom) (25% thermal ellipsoids; hydrogen atoms omitted; cyclohexyl groups shown as wireframe for clarity). See text for relevant bond lengths.

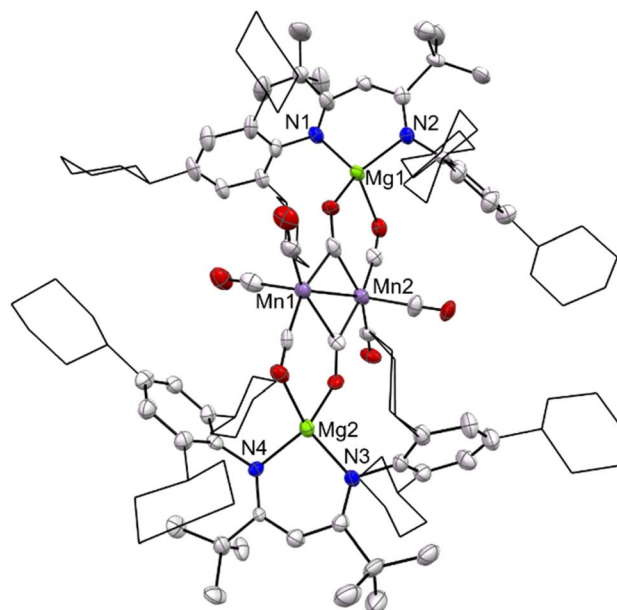


Fig. 7 Molecular structure of **11** (25% thermal ellipsoids; hydrogen atoms omitted; cyclohexyl groups shown as wireframe for clarity). See text for relevant bond lengths.

The molecular structures of **9** and **10** are depicted in Fig. 6. They reveal each to have a central  $[M_2(CO)_{10}]^{2-}$  ( $M = Cr$  or  $Mo$ ) dianion which bridges two  $[[TCHPNaacnac]Mg]^+$  counter-cations. The major difference between the compounds is that in the dianion of **9**, the two Cr centres are bridged by two CO ligands, which, as far as we are aware, is unknown for any dianion  $[M_2(CO)_{10}]^{2-}$  involving a group 6 metal.<sup>22</sup> Due to the carbonyl bridging in **9**, its Cr–Cr bond is markedly shorter (2.7659(13) Å) than in all other  $[Cr_2(CO)_{10}]^{2-}$  dianions, which have bond lengths of ca. 2.9–3.0 Å.<sup>22</sup> With that said, the Cr–Cr bond length in **9** lies comfortably within the known single bonded range for

noteworthy that **11** can also be formed in low yield from reaction of **6** with  $BrMn(CO)_5$ , yielding NaBr as a by-product. In addition, when the reactions giving **9–12** were carried out under an atmosphere of CO, instead of  $N_2$ , the same products formed in similar yields.

All compounds **9–12** are very air sensitive, but are indefinitely stable under inert atmospheres at room temperature. Although the compounds were crystallised from hexane solutions of the total reaction mixtures, once crystallised they showed negligible solubility in aliphatic or aromatic solvents. Moreover, attempts to dissolve them in ethereal solvents led to decomposition of the compounds as they were drawn into solution. Accordingly, no meaningful NMR spectroscopic data could be obtained for the compounds. However, the solid-state FTIR spectra for the compounds were acquired. In all cases, these exhibit complex patterns of CO stretching bands at frequencies consistent with the presence of both terminal and bridging CO ligands, as might be expected from the solid-state structures of the compounds (see below).

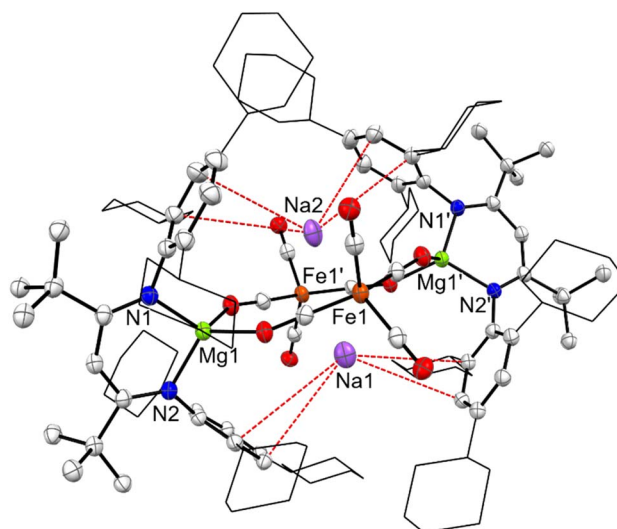


Fig. 8 Molecular structure of **12** (25% thermal ellipsoids; hydrogen atoms omitted; cyclohexyl groups shown as wireframe for clarity).



such bonds.<sup>22</sup> In contrast, the Mo–Mo single bond distance in **10** (3.101(5) Å) is close to those in all examples of the  $[\text{Mo}_2(\text{CO})_{10}]^{2-}$  dianion (range: 3.08 to 3.15 Å for 6 examples).<sup>22,23</sup> Another difference between **9** and **10** is the manner in which the  $[\text{M}_2(\text{CO})_{10}]^{2-}$  dianion bridges the two  $[(\text{TCHP}\text{Nacnac})\text{Mg}]^+$  cations. In **9** it does this by chelating each cation through the *O*-centres of both a Cr–Cr bridging and non-bridged CO ligand, whereas in **10** *O*-atoms from a non-bridging CO ligand on each Mo centre chelate an Mg atom.

The solid-state structure of **11** is displayed in Fig. 7. Similar to the structures of **9** and **10**, it exhibits a bridging  $[\text{Mn}_2(\text{CO})_8]^{2-}$  dianion. Another similarity with **9** is the fact that in **11** the central anion chelates each  $[(\text{TCHP}\text{Nacnac})\text{Mg}]^+$  cation through the *O*-centres of both a bridging and non-bridged CO ligand. However, in contrast to the Cr–Cr single bond in **9**, compound **11** exhibits an Mn=Mn double bond (2.460(2) Å). This is close to that for the free  $[\text{Mn}_2(\text{CO})_8]^{2-}$  dianion (2.5053(5) Å), which was first reported only recently, and which also possesses two bridging CO ligands.<sup>24,25</sup>

The product from the reduction of  $\text{Fe}(\text{CO})_5$  with magnesium(0) complex **6**, *viz.* **12**, differs from **9–11** in that it incorporates sodium cations in its structure (Fig. 8), and does not possess a metal–metal bond. Instead, it has two tetrahedral  $[\text{Fe}(\text{CO})_4]^{2-}$  dianions, both of which coordinate each  $[(\text{TCHP}\text{Nacnac})\text{Mg}]^+$  cation through two CO *O*-centres, with charge balance being provided by two central sodium cations. These have weak interactions with central arene rings of TCHP groups on both ligands, and lie close to both  $[\text{Fe}(\text{CO})_4]^{2-}$  dianions (mean  $\text{Na}\cdots\text{Fe}$  distance: 3.12 Å). Compound **12** can be thought of as an analogue of Collman's reagent,  $\text{Na}_2[\text{Fe}(\text{CO})_4]$ ,<sup>26</sup> in which one sodium cation is replaced with a  $[(\text{TCHP}\text{Nacnac})\text{Mg}]^+$  unit.

## Conclusions

In summary, three new very bulky  $\beta$ -diketimine proto-ligands ( $\text{ArNacnacH}$ , Ar = TCHP, DCHP or TCHP/Dip) have been synthesised and shown to exist as their diimine tautomers in the solid state and/or in solution. Several synthetic routes have been utilised to access monomeric, three-coordinate  $\beta$ -diketiminato magnesium iodide complexes, **1**, **3** and **5**, from the  $\beta$ -diketimines. Reduction of  $[(\text{TCHP}\text{Nacnac})\text{MgI}]$  **1** with 5% w/w Na/NaCl afforded the anionic magnesium(0) complex  $[(\text{TCHP}\text{Nacnac})\text{Mg}\text{Na}]_2$  **6**, which is closely related to the only other example of such a compound **III**, but can be formed in higher yield, and appears to be more thermally robust than **III**. In contrast, sodium reductions of impure samples of less bulky  $[(\text{DCHP}\text{Nacnac})\text{MgI}]$  **3** gave intractable product mixtures, whilst reduction of unsymmetrically substituted  $[(\text{TCHP}/\text{Dip}\text{Nacnac})\text{MgI}]$  **5** afforded the mixed oxidation state, linear tri-magnesium compound,  $[(\text{TCHP}/\text{Dip}\text{Nacnac})\text{Mg}]_2\text{Mg}$  **7**. A bulkier counterpart of this system,  $[(\text{TCHP}\text{Nacnac})\text{Mg}]_2\text{Mg}$  **8**, was prepared by sodium reduction of a 2 : 1 mixture of  $[(\text{TCHP}\text{Nacnac})\text{MgI}]$  **1** and  $\text{MgI}_2$ . Detailed computational analyses of compounds **6** and **8** revealed their electronic structures to be similar to those of **III** and **IV**, respectively.

Reactions of magnesium(0) compound **6** with the neutral groups **6–8** transition metal carbonyls,  $\text{Cr}(\text{CO})_6$ ,  $\text{Mo}(\text{CO})_6$ ,

$\text{Mn}_2(\text{CO})_{10}$  or  $\text{Fe}(\text{CO})_5$ , were subsequently carried out, in order to ascertain if these would lead to CO reductive homologation reactions. Instead, all reactions proceeded *via* reduction of the metal carbonyl reactant, which in the case of the group **6** and **7** metal carbonyls gave the complexes  $[(\text{TCHP}\text{Nacnac})\text{Mg}]_2\{\mu\text{-M}_2(\text{CO})_n\}$  ( $n = 10$ , M = Cr **9** or Mo **10**;  $n = 8$ , M = Mn **11**), which incorporate dianionic metal–metal single (**9** and **10**) or double (**11**) bonded metal carbonyl fragments. The bonding modes within these fragments, and to the coordinated  $[(\text{TCHP}\text{Nacnac})\text{Mg}]^+$  cations, varies across the trio of compounds. In contrast to the formations of **9–11**, reduction of  $\text{Fe}(\text{CO})_5$  with **6** did not proceed with loss of sodium, instead giving  $[(\text{TCHP}\text{Nacnac})\text{Mg}\text{Na}\{\text{Fe}(\text{CO})_4\}]_2$  **12**. This resembles Collman's reagent, in that it incorporates  $[\text{Fe}(\text{CO})_4]^{2-}$  dianions. We continue to explore the reduction chemistry of magnesium(0) compounds such as **6–8**, and will report on our efforts in this direction in due course.

## Experimental section

Full synthetic, spectroscopic and crystallographic details for new compounds; and full details and references for the calculations can be found in the SI.

## Author contributions

C. J. conceived and designed the experiments; Y. J., M. N., S. G. U. and M. J. E. performed the experiments; J. M. P. carried out the computational studies; all authors analysed the data; C. J. wrote the manuscript; all authors revised and edited the manuscript; all authors have read and agreed to the published version of the manuscript.

## Conflicts of interest

There are no conflicts of interest to declare.

## Data availability

CCDC 2534925–2534941 contain the supplementary crystallographic data for this paper.<sup>27a–q</sup>

Data supporting this article have been included as part of the supplementary information (SI). Supplementary information is available. See DOI: <https://doi.org/10.1039/d6sc01992g>.

## Acknowledgements

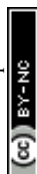
CJ thanks the Australian Research Council and the US Air Force Asian Office of Aerospace Research and Development (grant FA2386-21-1-4048) for generous funding. We also wish to acknowledge the Australian Synchrotron for access to their MX1 and MX2 beamlines.

## Notes and references

- Selected reviews on low oxidation state p-block compounds and their reactivity(a) C. Weetman and S. Inoue, *ChemCatChem*, 2018, **10**, 4213–4228; (b) T. Chu and



- G. I. Nikonov, *Chem. Rev.*, 2018, **118**, 3608–3680; (c) T. J. Hadlington, M. Driess and C. Jones, *Chem. Soc. Rev.*, 2018, **47**, 4176–4197; (d) S. S. Sen, S. Khan, P. P. Samuel and H. W. Roesky, *Chem. Sci.*, 2012, **3**, 659–682; (e) P. P. Power, *Acc. Chem. Res.*, 2011, **44**, 627–637; (f) P. P. Power, *Nature*, 2010, **463**, 171–177; (g) S. Yadav, S. Saha and S. S. Sen, *ChemCatChem*, 2016, **8**, 486–501; (h) J. Hicks, P. Vasko, J. M. Goicoechea and S. Aldridge, *Angew. Chem., Int. Ed.*, 2021, **60**, 1702–1713; (i) M. Asay, C. Jones and M. Driess, *Chem. Rev.*, 2011, **111**, 354–396; (j) S. Fujimori and S. Inoue, *Eur. J. Inorg. Chem.*, 2020, **2020**, 3131–3142; (k) H. W. Moon and J. Cornella, *ACS Catal.*, 2022, **12**, 1382–1393; (l) J. M. Lipshultz, G. Li and A. T. Radosevich, *J. Am. Chem. Soc.*, 2021, **143**, 1699–1721; (m) M. Mato and J. Cornella, *Angew. Chem., Int. Ed.*, 2024, **63**, e202315046; (n) M. P. Coles and M. J. Evans, *Chem. Commun.*, 2023, **59**, 503–519.
- 2 S. P. Green, C. Jones and A. Stasch, *Science*, 2007, **318**, 1754–1757.
- 3 Selected reviews on low oxidation state group 2 metal compounds and their reactivity (a) C. Jones, *Nat. Rev. Chem.*, 2017, **1**, 0059; (b) A. Stasch and C. Jones, *Dalton Trans.*, 2011, **40**, 5659–5672; (c) B. Rösch and S. Harder, *Chem. Commun.*, 2021, **57**, 9354–9365; (d) L. A. Freeman, J. E. Walley and R. J. Gilliard, *Nat. Synth.*, 2022, **1**, 439–448; (e) M. J. Evans and C. Jones, *Chem. Soc. Rev.*, 2024, **53**, 5054–5082; (f) S. Kriek, L. Yu, M. Reiher and M. Westerhausen, *Eur. J. Inorg. Chem.*, 2010, **2010**, 197–216; (g) J. T. Boronski, *Dalton Trans.*, 2024, **53**, 33–39.
- 4 R. Mondal, M. J. Evans, D. T. Nguyen, T. Rajeshkumar, L. Maron and C. Jones, *Chem. Commun.*, 2024, **60**, 1016–1019.
- 5 C. Jones, *Commun. Chem.*, 2020, **3**, 159.
- 6 (a) B. Rösch, T. X. Gentner, J. Eyselien, J. Langer, H. Elsen and S. Harder, *Nature*, 2021, **592**, 717–721; (b) C. Jones, *Nature*, 2021, **592**, 687–688.
- 7 (a) J. Mai, J. Maurer, J. Langer and S. Harder, *Nat. Synth.*, 2024, **3**, 368–377; (b) S. K. Thakur, J. Langer, N. Roig, A. G. Patro, M. A. Schmidt, M. Alonso and S. Harder, *Angew. Chem., Int. Ed.*, 2026, **65**, e25777; (c) J. Mai, B. Rösch, N. Patel, J. Langer and S. Harder, *Chem. Sci.*, 2023, **14**, 4724–4734; (d) C. Berthold, J. Maurer, L. Klerner, S. Harder and M. R. Buchner, *Angew. Chem., Int. Ed.*, 2024, **63**, e202408422; (e) J. Maurer, J. Langer, J. Mai, M. A. Schmidt, C. Färber, L. Klerner, T. Vilpas, M. H. Linden, H. B. Linden, A. Koldemir, J. Wiethölter, R. Pöttgen, S. Harder, *Nat. Synth.*, in press online article, DOI: [10.1038/s44160-026-01006-7](https://doi.org/10.1038/s44160-026-01006-7).
- 8 S. K. Thakur, N. Roig, J. Maurer, J. Langer, M. Alonso and S. Harder, *J. Am. Chem. Soc.*, 2025, **147**, 12555–12561.
- 9 J. Maurer, L. Klerner, J. Mai, H. Stecher, S. Thum, M. Morasch, J. Langer and S. Harder, *Nat. Chem.*, 2025, **17**, 703–709.
- 10 R. Mondal, K. Yuvaraj, T. Rajeshkumar, L. Maron and C. Jones, *Chem. Commun.*, 2022, **58**, 12665–12668.
- 11 R. Mondal, M. J. Evans, T. Rajeshkumar, L. Maron and C. Jones, *Angew. Chem., Int. Ed.*, 2023, **62**, e202308347.
- 12 K. Yuvaraj, I. Douair, D. D. L. Jones, L. Maron and C. Jones, *Chem. Sci.*, 2020, **11**, 3516–3522.
- 13 T. X. Gentner, B. Rösch, G. Ballmann, J. Langer, H. Elsen and S. Harder, *Angew. Chem., Int. Ed.*, 2019, **58**, 607–611.
- 14 P. H. M. Budzelaar, A. B. van Oort and A. G. Orpen, *Eur. J. Inorg. Chem.*, 1998, **1998**, 1485–1494.
- 15 B. Rosch, T. X. Gentner, J. Eyselien, A. Friedrich, J. Langer and S. Harder, *Chem. Commun.*, 2020, **56**, 11402–11405.
- 16 M. Arrowsmith, B. Maitland, G. Kociok-Kohn, A. Stasch, C. Jones and M. S. Hill, *Inorg. Chem.*, 2014, **53**, 10543–10552.
- 17 S. J. Bonyhady, C. Jones, S. Nembenna, A. Stasch, A. J. Edwards and G. J. McIntyre, *Chem. – Eur. J.*, 2010, **16**, 938–955.
- 18 J. Hicks, M. Juckel, A. Paparo, D. Dange and C. Jones, *Organometallics*, 2018, **37**, 4810–4813.
- 19 (a) J. A. Platts, J. Overgaard, C. Jones, B. B. Iverson and A. Stasch, *J. Phys. Chem. A*, 2011, **115**, 194–200; (b) L.-C. Wu, C. Jones, A. Stasch, J. A. Platts and J. Overgaard, *Eur. J. Inorg. Chem.*, 2014, **2014**, 5536–5540.
- 20 (a) K. Yuvaraj, I. Douair, A. Paparo, L. Maron and C. Jones, *J. Am. Chem. Soc.*, 2019, **141**, 8764–8768; (b) K. Yuvaraj, J. C. Mullins, T. Rajeshkumar, I. Douair, L. Maron and C. Jones, *Chem. Sci.*, 2023, **14**, 5188–5195; (c) D. T. Nguyen, R. Mondal, M. J. Evans, J. M. Parr and C. Jones, *Angew. Chem., Int. Ed.*, 2025, **137**, e202500264.
- 21 A. Paparo, K. Yuvaraj, A. J. R. Matthews, I. Douair, L. Maron and C. Jones, *Angew. Chem., Int. Ed.*, 2021, **60**, 630–634.
- 22 As determined from a survey of the Cambridge Crystallographic Database, 2026.
- 23 See, for example: L. B. Handy, J. K. Ruff and L. F. Dahl, *J. Am. Chem. Soc.*, 1970, **92**, 7312–7326.
- 24 M. Witzmann, F. Wieberneit and N. Korber, *Z. Anorg. Allg. Chem.*, 2026, **652**, e202500172.
- 25 J. A. Baus, J. Poater, F. M. Bickelhaupt and R. Tacke, *Eur. J. Inorg. Chem.*, 2017, **2017**, 186–191.
- 26 J. P. Collman, *Acc. Chem. Res.*, 1975, **8**, 342–347.
- 27 (a) CCDC 2534925: Experimental Crystal Structure Determination, 2026, DOI: [10.5517/ccdc.csd.cc2r2ssf](https://doi.org/10.5517/ccdc.csd.cc2r2ssf); (b) CCDC 2534926: Experimental Crystal Structure Determination, 2026, DOI: [10.5517/ccdc.csd.cc2r2stg](https://doi.org/10.5517/ccdc.csd.cc2r2stg); (c) CCDC 2534927: Experimental Crystal Structure Determination, 2026, DOI: [10.5517/ccdc.csd.cc2r2svh](https://doi.org/10.5517/ccdc.csd.cc2r2svh); (d) CCDC 2534928: Experimental Crystal Structure Determination, 2026, DOI: [10.5517/ccdc.csd.cc2r2swj](https://doi.org/10.5517/ccdc.csd.cc2r2swj); (e) CCDC 2534929: Experimental Crystal Structure Determination, 2026, DOI: [10.5517/ccdc.csd.cc2r2sxx](https://doi.org/10.5517/ccdc.csd.cc2r2sxx); (f) CCDC 2534930: Experimental Crystal Structure Determination, 2026, DOI: [10.5517/ccdc.csd.cc2r2syt](https://doi.org/10.5517/ccdc.csd.cc2r2syt); (g) CCDC 2534931: Experimental Crystal Structure Determination, 2026, DOI: [10.5517/ccdc.csd.cc2r2szm](https://doi.org/10.5517/ccdc.csd.cc2r2szm); (h) CCDC 2534932: Experimental Crystal Structure Determination, 2026, DOI: [10.5517/ccdc.csd.cc2r2t0p](https://doi.org/10.5517/ccdc.csd.cc2r2t0p); (i) CCDC 2534933: Experimental Crystal Structure Determination, 2026, DOI: [10.5517/ccdc.csd.cc2r2t1q](https://doi.org/10.5517/ccdc.csd.cc2r2t1q); (j) CCDC 2534934: Experimental Crystal Structure Determination, 2026, DOI: [10.5517/ccdc.csd.cc2r2t2r](https://doi.org/10.5517/ccdc.csd.cc2r2t2r); (k) CCDC 2534935: Experimental Crystal Structure



Determination, 2026, DOI: [10.5517/ccdc.csd.cc2r2t3s](https://doi.org/10.5517/ccdc.csd.cc2r2t3s); (*l*)  
CCDC 2534936: Experimental Crystal Structure  
Determination, 2026, DOI: [10.5517/ccdc.csd.cc2r2t4t](https://doi.org/10.5517/ccdc.csd.cc2r2t4t); (*m*)  
CCDC 2534937: Experimental Crystal Structure  
Determination, 2026, DOI: [10.5517/ccdc.csd.cc2r2t5v](https://doi.org/10.5517/ccdc.csd.cc2r2t5v); (*n*)  
CCDC 2534938: Experimental Crystal Structure  
Determination, 2026, DOI: [10.5517/ccdc.csd.cc2r2t6w](https://doi.org/10.5517/ccdc.csd.cc2r2t6w); (*o*)

CCDC 2534939: Experimental Crystal Structure  
Determination, 2026, DOI: [10.5517/ccdc.csd.cc2r2t7x](https://doi.org/10.5517/ccdc.csd.cc2r2t7x); (*p*)  
CCDC 2534940: Experimental Crystal Structure  
Determination, 2026, DOI: [10.5517/ccdc.csd.cc2r2t8y](https://doi.org/10.5517/ccdc.csd.cc2r2t8y); (*q*)  
CCDC 2534941: Experimental Crystal Structure  
Determination, 2026, DOI: [10.5517/ccdc.csd.cc2r2t9z](https://doi.org/10.5517/ccdc.csd.cc2r2t9z).

